

# Northumbria Research Link

Citation: Vo, Thuc and Thai, Huu-Tai (2012) Free vibration of axially loaded rectangular composite beams using refined shear deformation theory. Composite Structures, 94 (11). 3379 - 3387. ISSN 0263-8223

Published by: Elsevier

URL: <http://dx.doi.org/10.1016/j.compstruct.2012.05.012>  
<<http://dx.doi.org/10.1016/j.compstruct.2012.05.012>>

This version was downloaded from Northumbria Research Link:  
<http://nrl.northumbria.ac.uk/id/eprint/13376/>

Northumbria University has developed Northumbria Research Link (NRL) to enable users to access the University's research output. Copyright © and moral rights for items on NRL are retained by the individual author(s) and/or other copyright owners. Single copies of full items can be reproduced, displayed or performed, and given to third parties in any format or medium for personal research or study, educational, or not-for-profit purposes without prior permission or charge, provided the authors, title and full bibliographic details are given, as well as a hyperlink and/or URL to the original metadata page. The content must not be changed in any way. Full items must not be sold commercially in any format or medium without formal permission of the copyright holder. The full policy is available online: <http://nrl.northumbria.ac.uk/policies.html>

This document may differ from the final, published version of the research and has been made available online in accordance with publisher policies. To read and/or cite from the published version of the research, please visit the publisher's website (a subscription may be required.)



**Northumbria  
University**  
NEWCASTLE



**UniversityLibrary**

# Free vibration of axially loaded rectangular composite beams using refined shear deformation theory

Thuc P. Vo<sup>a,b,\*</sup>, Huu-Tai Thai<sup>c</sup>

<sup>a</sup>*School of Mechanical, Aeronautical and Electrical Engineering, Glyndŵr University, Mold Road, Wrexham LL11 2AW, UK.*

<sup>b</sup>*Advanced Composite Training and Development Centre, Glyndŵr University, Unit 5, Hawarden Industrial Park, Deeside, Flintshire CH5 3US, UK.*

<sup>c</sup>*Department of Civil and Environmental Engineering, Hanyang University, 17 Haengdang-dong, Seongdong-gu, Seoul 133-791, Republic of Korea.*

---

## Abstract

Free vibration of axially loaded rectangular composite beams with arbitrary lay-ups using refined shear deformation theory is presented. It accounts for the parabolical variation of shear strains through the depth of beam. Three governing equations of motion are derived from the Hamilton's principle. The resulting coupling is referred to as triply axial-flexural coupled vibration. A displacement-based one-dimensional finite element model is developed to solve the problem. Numerical results are obtained for rectangular composite beams to investigate effects of fiber orientation and modulus ratio on the natural frequencies, critical buckling loads and load-frequency curves as well as corresponding mode shapes.

**Keywords:** Refined shear deformation theory; triply axial-flexural coupled vibration; load-frequency curves.

---

## 1. Introduction

Structural components made with composite materials are increasingly being used in various engineering applications due to their attractive properties in strength, stiffness, and lightness. Understanding their dynamic behaviour is of increasing importance. [For some practical applications, earlier research on the free vibration characteristics of metallic beams \(\[1\], \[2\]\) has shown that the effects of axial force on natural frequencies and mode shapes are, in general, much more pronounced than those of the shear deformation and/or rotatory inertia.](#) Thanks to the advantage that no shear correction factors are needed, the higher-order beam theory (HOBT) is widely used for analysis of composite beams. Though many works on dynamic characteristics are available in the open literature ([3]- [12]), only representative samples are cited here, while detailed discussions can be found in Ref. [13]. Some

---

\*Corresponding author, tel.: +44 1978 293979  
Email address: [t.vo@glyndwr.ac.uk](mailto:t.vo@glyndwr.ac.uk) (Thuc P. Vo)

researchers studied vibration and buckling problems in a unified fashion ([14]-[20]). Although a large number of studies have been performed on these problems of composite beams using HOBTs, there appear to be few papers that reported on the free vibration of axially loaded composite beams. Jun and Hongxing [13] introduced the dynamic stiffness matrix method to solve the free vibration of axially loaded composite beams with arbitrary lay-ups. Karama et al. [21] presented static and dynamic of composite beams with a transverse shear stress continuity model based on trigonometric shear deformation theory.

In this paper, which is extended from previous research [22], free vibration of axially loaded rectangular composite beams with arbitrary lay-ups using refined shear deformation theory is presented. It accounts for the parabolical variation of shear strains through the depth of beam. Three governing equations of motion are derived from the Hamilton's principle. The resulting coupling is referred to as triply axial-flexural coupled vibration. A displacement-based one-dimensional finite element model is developed to solve the problem. Numerical results are obtained for composite beams to investigate effects of fiber orientation and modulus ratio on the natural frequencies, critical buckling loads and load-frequency curves as well as corresponding mode shapes.

## 2. Kinematics

Consider a laminated composite beam with length  $L$  and rectangular cross-section  $b \times h$ , with  $b$  being the width and  $h$  being the height. The  $x$ -,  $y$ -, and  $z$ -axes are taken along the length, width, and height of the beam, respectively. This composite beams is made of many plies of orthotropic materials in different orientations with respect to the  $x$ -axis. To derive the finite element model of composite beam, the following assumptions are made for the displacement field:

- (a) The axial and transverse displacements consist of bending and shear components in which the bending component does not contribute toward shear forces and, likewise, the shear component does not contribute toward bending moments.
- (b) The bending component of axial displacement is similar to that given by the Euler-Bernoulli beam theory.
- (c) The shear component of axial displacement gives rise to the higher-order variation of shear strain and hence to shear stress through the depth of the beam in such a way that shear stress vanishes on the top and bottom surfaces.

The displacement field of the present theory can be obtained as:

$$U(x, z, t) = u(x, t) - z \frac{\partial w_b(x, t)}{\partial x} + z \left[ \frac{1}{4} - \frac{5}{3} \left( \frac{z}{h} \right)^2 \right] \frac{\partial w_s(x, t)}{\partial x} \quad (1a)$$

$$W(x, z, t) = w_b(x, t) + w_s(x, t) \quad (1b)$$

where  $u$  is the axial displacement along the mid-plane of the beam,  $w_b$  and  $w_s$  are the bending and shear components of transverse displacement along the mid-plane of the beam, respectively. The non-zero strains are given by:

$$\epsilon_x = \frac{\partial U}{\partial x} = \epsilon_x^\circ + z \kappa_x^b + f \kappa_x^s \quad (2a)$$

$$\gamma_{xz} = \frac{\partial W}{\partial x} + \frac{\partial U}{\partial z} = (1 - f') \gamma_{xz}^\circ = g \gamma_{xz}^\circ \quad (2b)$$

where

$$f = z \left[ -\frac{1}{4} + \frac{5}{3} \left( \frac{z}{h} \right)^2 \right] \quad (3a)$$

$$g = 1 - f' = \frac{5}{4} \left[ 1 - 4 \left( \frac{z}{h} \right)^2 \right] \quad (3b)$$

and  $\epsilon_x^\circ$ ,  $\gamma_{xz}^\circ$ ,  $\kappa_x^b$ ,  $\kappa_x^s$  and  $\kappa_{xy}$  are the axial strain, shear strains and curvatures in the beam, respectively defined as:

$$\epsilon_x^\circ = u' \quad (4a)$$

$$\gamma_{xz}^\circ = w_s' \quad (4b)$$

$$\kappa_x^b = -w_b'' \quad (4c)$$

$$\kappa_x^s = -w_s'' \quad (4d)$$

where differentiation with respect to the  $x$ -axis is denoted by primes ( $'$ ).

### 3. Variational Formulation

In order to derive the equations of motion, Hamilton's principle is used:

$$\delta \int_{t_1}^{t_2} (\mathcal{K} - \mathcal{U} - \mathcal{V}) dt = 0 \quad (5)$$

where  $\mathcal{U}$  is the variation of the strain energy,  $\mathcal{V}$  is the variation of the potential energy, and  $\mathcal{K}$  is the variation of the kinetic energy.

The variation of the strain energy can be stated as:

$$\delta \mathcal{U} = \int_v (\sigma_x \delta \epsilon_x + \sigma_{xz} \delta \gamma_{xz}) dv = \int_0^l (N_x \delta \epsilon_x^\circ + M_x^b \delta \kappa_x^b + M_x^s \delta \kappa_x^s + Q_{xz} \delta \gamma_{xz}^\circ) dx \quad (6)$$

where  $N_x, M_x^b, M_x^s$  and  $Q_{xz}$  are the axial force, bending moments and shear force, respectively, defined by integrating over the cross-sectional area  $A$  as:

$$N_x = \int_A \sigma_x dA \quad (7a)$$

$$M_x^b = \int_A \sigma_x z dA \quad (7b)$$

$$M_x^s = \int_A \sigma_x f dA \quad (7c)$$

$$Q_{xz} = \int_A \sigma_{xz} g dA \quad (7d)$$

The variation of the potential energy of the axial force can be expressed as:

$$\delta \mathcal{V} = - \int_0^l P_0 \left[ \delta w_b' (w_b' + w_s') + \delta w_s' (w_b' + w_s') \right] dx \quad (8)$$

The variation of the kinetic energy is obtained as:

$$\begin{aligned} \delta \mathcal{K} &= \int_v \rho_k (\dot{U} \delta \dot{U} + \dot{W} \delta \dot{W}) dv \\ &= \int_0^l \left[ \delta \dot{u} (m_0 \dot{u} - m_1 \dot{w}_b' - m_f \dot{w}_s') + \delta \dot{w}_b m_0 (\dot{w}_b + \dot{w}_s) + \delta \dot{w}_b' (-m_1 \dot{u} + m_2 \dot{w}_b' + m_{fz} \dot{w}_s') \right. \\ &\quad \left. + \delta \dot{w}_s m_0 (\dot{w}_b + \dot{w}_s) + \delta \dot{w}_s' (-m_f \dot{u} + m_{fz} \dot{w}_b' + m_{f2} \dot{w}_s') \right] dx \end{aligned} \quad (9)$$

where the differentiation with respect to the time  $t$  is denoted by dot-superscript convention;  $\rho_k$  is the density of a  $k^{th}$  layer and  $m_0, m_1, m_2, m_f, m_{fz}$  and  $m_{f2}$  are the inertia coefficients, defined by:

$$m_f = -\frac{m_1}{4} + \frac{5}{3h^2} m_3 \quad (10a)$$

$$m_{fz} = -\frac{m_2}{4} + \frac{5}{3h^2} m_4 \quad (10b)$$

$$m_{f2} = \frac{m_2}{16} - \frac{5}{6h^2} m_4 + \frac{25}{9h^4} m_6 \quad (10c)$$

where

$$(m_0, m_1, m_2, m_3, m_4, m_6) = \int_A \rho_k (1, z, z^2, z^3, z^4, z^6) dA \quad (11)$$

By substituting Eqs. (6), (8) and (9) into Eq. (5), the following weak statement is obtained:

$$\begin{aligned} 0 &= \int_{t_1}^{t_2} \int_0^l \left[ \delta \dot{u} (m_0 \dot{u} - m_1 \dot{w}_b' - m_f \dot{w}_s') + \delta \dot{w}_b m_0 (\dot{w}_b + \dot{w}_s) + \delta \dot{w}_b' (-m_1 \dot{u} + m_2 \dot{w}_b' + m_{fz} \dot{w}_s') \right. \\ &\quad + \delta \dot{w}_s m_0 (\dot{w}_b + \dot{w}_s) + \delta \dot{w}_s' (-m_f \dot{u} + m_{fz} \dot{w}_b' + m_{f2} \dot{w}_s') \\ &\quad \left. + P_0 [\delta w_b' (w_b' + w_s') + \delta w_s' (w_b' + w_s')] - N_x \delta u' + M_x^b \delta w_b'' + M_x^s \delta w_s'' - Q_{xz} \delta w_s' \right] dx dt \end{aligned} \quad (12)$$

#### 4. Constitutive Equations

The stress-strain relations for the  $k^{th}$  lamina are given by:

$$\sigma_x = \bar{Q}_{11}\epsilon_x \quad (13a)$$

$$\sigma_{xz} = \bar{Q}_{55}\gamma_{xz} \quad (13b)$$

where  $\bar{Q}_{11}$  and  $\bar{Q}_{55}$  are the elastic stiffnesses transformed to the  $x$  direction. More detailed explanation can be found in Ref. [23].

The constitutive equations for bar forces and bar strains are obtained by using Eqs. (2), (7) and (13):

$$\begin{Bmatrix} N_x \\ M_x^b \\ M_x^s \\ Q_{xz} \end{Bmatrix} = \begin{bmatrix} R_{11} & R_{12} & R_{13} & 0 \\ & R_{22} & R_{23} & 0 \\ & & R_{33} & 0 \\ \text{sym.} & & & R_{44} \end{bmatrix} \begin{Bmatrix} \epsilon_x^\circ \\ \kappa_x^b \\ \kappa_x^s \\ \gamma_{xz}^\circ \end{Bmatrix} \quad (14)$$

where  $R_{ij}$  are the laminate stiffnesses of general composite beams and given by:

$$R_{11} = \int_y A_{11} dy \quad (15a)$$

$$R_{12} = \int_y B_{11} dy \quad (15b)$$

$$R_{13} = \int_y \left(-\frac{B_{11}}{4} + \frac{5}{3h^2}E_{11}\right) dy \quad (15c)$$

$$R_{22} = \int_y D_{11} dy \quad (15d)$$

$$R_{23} = \int_y \left(-\frac{D_{11}}{4} + \frac{5}{3h^2}F_{11}\right) dy \quad (15e)$$

$$R_{33} = \int_y \left(\frac{D_{11}}{16} - \frac{5}{6h^2}F_{11} + \frac{25}{9h^4}H_{11}\right) dy \quad (15f)$$

$$R_{44} = \int_y \left(\frac{25}{16}A_{55} - \frac{25}{2h^2}D_{55} + \frac{25}{h^4}F_{55}\right) dy \quad (15g)$$

where  $A_{ij}$ ,  $B_{ij}$  and  $D_{ij}$  matrices are the extensional, coupling and bending stiffness and  $E_{ij}$ ,  $F_{ij}$ ,  $H_{ij}$  matrices are the higher-order stiffnesses, respectively, defined by:

$$(A_{ij}, B_{ij}, D_{ij}, E_{ij}, F_{ij}, H_{ij}) = \int_z \bar{Q}_{ij}(1, z, z^2, z^3, z^4, z^6) dz \quad (16)$$

## 5. Governing equations of motion

The equilibrium equations of the present study can be obtained by integrating the derivatives of the varied quantities by parts and collecting the coefficients of  $\delta u$ ,  $\delta w_b$  and  $\delta w_s$ :

$$N'_x = m_0\ddot{u} - m_1\ddot{w}_b' - m_f\ddot{w}_s' \quad (17a)$$

$$M_x^{b''} - P_0(w_b'' + w_s'') = m_0(\ddot{w}_b + \ddot{w}_s) + m_1\ddot{u}' - m_2\ddot{w}_b'' - m_{fz}\ddot{w}_s'' \quad (17b)$$

$$M_x^{s''} + Q'_{xz} - P_0(w_b'' + w_s'') = m_0(\ddot{w}_b + \ddot{w}_s) + m_f\ddot{u}' - m_{fz}\ddot{w}_b'' - m_{f2}\ddot{w}_s'' \quad (17c)$$

The natural boundary conditions are of the form:

$$\delta u : N_x \quad (18a)$$

$$\delta w_b : M_x^{b'} - P_0(w_b' + w_s') - m_1\ddot{u} + m_2\ddot{w}_b' + m_{fz}\ddot{w}_s' \quad (18b)$$

$$\delta w_b' : M_x^b \quad (18c)$$

$$\delta w_s : M_x^{s'} + Q_{xz} - P_0(w_b' + w_s') - m_f\ddot{u} + m_{fz}\ddot{w}_b' + m_{f2}\ddot{w}_s' \quad (18d)$$

$$\delta w_s' : M_x^s \quad (18e)$$

By substituting Eqs. (4) and (14) into Eq. (17), the explicit form of the governing equations of motion can be expressed with respect to the laminate stiffnesses  $R_{ij}$ :

$$R_{11}u'' - R_{12}w_b''' - R_{13}w_s''' = m_0\ddot{u} - m_1\ddot{w}_b' - m_f\ddot{w}_s' \quad (19a)$$

$$\begin{aligned} R_{12}u''' - R_{22}w_b^{iv} - R_{23}w_s^{iv} - P_0(w_b'' + w_s'') &= m_0(\ddot{w}_b + \ddot{w}_s) + m_1\ddot{u}' \\ &- m_2\ddot{w}_b'' - m_{fz}\ddot{w}_s'' \end{aligned} \quad (19b)$$

$$\begin{aligned} R_{13}u''' - R_{23}w_b^{iv} - R_{33}w_s^{iv} + R_{44}w_s'' - P_0(w_b'' + w_s'') &= m_0(\ddot{w}_b + \ddot{w}_s) + m_f\ddot{u}' \\ &- m_{fz}\ddot{w}_b'' - m_{f2}\ddot{w}_s'' \end{aligned} \quad (19c)$$

Eq. (19) is the most general form for the free vibration of axially loaded of rectangular composite beams with arbitrary lay-ups, and the dependent variables,  $u$ ,  $w_b$  and  $w_s$  are fully coupled.

## 6. Finite Element Formulation

The present theory for composite beams described in the previous section was implemented via a displacement based finite element method. The variational statement in Eq. (12) requires that the bending and shear components of transverse displacement  $w_b$  and  $w_s$  be twice differentiable and  $C^1$ -continuous, whereas the axial displacement  $u$  must be only once differentiable and  $C^0$ -continuous. The

generalized displacements are expressed over each element as a combination of the linear interpolation function  $\Psi_j$  for  $u$  and Hermite-cubic interpolation function  $\psi_j$  for  $w_b$  and  $w_s$  associated with node  $j$  and the nodal values:

$$u = \sum_{j=1}^2 u_j \Psi_j \quad (20a)$$

$$w_b = \sum_{j=1}^4 w_{bj} \psi_j \quad (20b)$$

$$w_s = \sum_{j=1}^4 w_{sj} \psi_j \quad (20c)$$

Substituting these expressions in Eq. (20) into the corresponding weak statement in Eq. (12), the finite element model of a typical element can be expressed as the standard eigenvalue problem:

$$([K] - P_0[G] - \omega^2[M])\{\Delta\} = \{0\} \quad (21)$$

where  $[K]$ ,  $[G]$  and  $[M]$  are the element stiffness matrix, the element geometric stiffness matrix and the element mass matrix, respectively. The explicit forms of  $[K]$  can be found in Ref. [22] and of  $[G]$  and  $[M]$  are given by:

$$G_{ij}^{22} = \int_0^l \psi'_i \psi'_j dz \quad (22a)$$

$$G_{ij}^{23} = \int_0^l \psi'_i \psi'_j dz \quad (22b)$$

$$G_{ij}^{33} = \int_0^l \psi'_i \psi'_j dz \quad (22c)$$

$$M_{ij}^{11} = \int_0^l m_0 \Psi_i \Psi_j dz \quad (22d)$$

$$M_{ij}^{12} = - \int_0^l m_1 \Psi_i \psi'_j dz \quad (22e)$$

$$M_{ij}^{13} = - \int_0^l m_f \Psi_i \psi'_j dz \quad (22f)$$

$$M_{ij}^{22} = \int_0^l m_0 \psi_i \psi_j + m_2 \psi'_i \psi'_j dz \quad (22g)$$

$$M_{ij}^{23} = \int_0^l m_0 \psi_i \psi_j + m_{fz} \psi'_i \psi'_j dz \quad (22h)$$

$$M_{ij}^{33} = \int_0^l m_0 \psi_i \psi_j + m_{f2} \psi'_i \psi'_j dz \quad (22i)$$

All other components are zero. In Eq. (21),  $\{\Delta\}$  is the eigenvector of nodal displacements corresponding to an eigenvalue:

$$\{\Delta\} = \{u \ w_b \ w_s\}^T \quad (23)$$



## 7. Numerical Examples

For verification purpose, vibration analysis of axially loaded simply-supported beam with a symmetric cross-ply  $[90^\circ/0^\circ/0^\circ/90^\circ]$  lay-up and span-to-height ( $L/h = 2.273$ ) is analysed first. Throughout the numerical examples, 20 Hermitian beam elements with 105 degrees of freedom are used. The material properties are assumed to be [21]:  $E_1 = 241.5\text{GPa}$ ,  $E_2 = 18.98\text{GPa}$ ,  $G_{12} = G_{13} = 5.18\text{GPa}$ ,  $G_{23} = 3.45\text{GPa}$ ,  $\nu_{12} = 0.24$ ,  $\rho = 2015\text{Kg/m}^3$ . The value of  $10^9$  N is adopted as initial compressive and tensile force. Effect of the axial force on the first four natural frequencies is displayed in Table 1. This table also shows a comparison with the numerical results given in previous studies, which were based on a family of sinus finite elements [10], trigonometric shear deformation theory [21] and the commercial software ABAQUS. A good agreement between the predictions of the present model and the earlier works can be seen.

Next, the natural frequencies of symmetric cross-ply  $[0^\circ/90^\circ/90^\circ/0^\circ]$  composite beam with  $L/h = 10$  are given for different boundary conditions in Table 2. The material properties of AS4/3501-6 graphite/epoxy composite are assumed to be [7]:  $E_1 = 144.9\text{GPa}$ ,  $E_2 = 9.65\text{GPa}$ ,  $G_{12} = G_{13} = 4.14\text{GPa}$ ,  $G_{23} = 3.45\text{GPa}$ ,  $\nu_{12} = 0.3$ . The non-dimensional term is defined by:  $\bar{\omega} = \frac{\omega L^2}{h} \sqrt{\frac{\rho}{E_1}}$ . It can be noticed that the natural frequencies given in Table 2 are in excellent agreement with the reference solution [7], which were also obtained from the higher-order beam theory, for all boundary conditions.

In the next example, simply-supported anti-symmetric cross-ply composite beams with different span-to-height ratios are considered. This example is issued from [10] and the material properties are:  $E_1 = 181.0\text{GPa}$ ,  $E_2 = 10.3\text{GPa}$ ,  $G_{12} = G_{13} = 7.17\text{GPa}$ ,  $G_{23} = 2.87\text{GPa}$ ,  $\nu_{12} = 0.3$ ,  $\rho = 1578\text{Kg/m}^3$ . The non-dimensional term is defined by:  $\bar{\omega} = \frac{\omega L^2}{h} \sqrt{\frac{\rho}{E_2}}$ . The first four natural frequencies are evaluated and compared with numerical results in Ref. [10] in Table 3. It is observed that the present results are in good agreement with previous study and the commercial software ANSYS for the thin and thick beam.

To demonstrate the accuracy and validity of this study further, symmetric and anti-symmetric cross-ply composite beams are considered. In the following examples, all laminate are of equal thickness and made of the same orthotropic material, whose properties are:

$$E_1/E_2 = 40, G_{12} = G_{13} = 0.6E_2, G_{23} = 0.5E_2, \nu_{12} = 0.25 \quad (24)$$

For convenience, the following non-dimensional natural frequencies and critical buckling loads are

used:

$$\overline{P}_{cr} = \frac{P_{cr} L^2}{E_2 b h^3} \quad (25a)$$

$$\overline{\omega} = \frac{\omega L^2}{h} \sqrt{\frac{\rho}{E_2}} \quad (25b)$$

The fundamental natural frequencies and critical buckling loads for different span-to-height ratios and different boundary conditions are compared with those of ([14], [15]), who used a state-space concept in conjunction with the Jordan canonical form to obtain exact solutions and previous results ([8], [18], [19]) in Tables 4 and 5. It should be noted that the numerical results given in Refs. ([8], [14], [15], [18], [19]) were obtained from different higher-order beam theories. Through the close correlation observed between the present model and the earlier works, accuracy and adequacy of the present model is again established.

In order to investigate the effects of the axial force, fiber orientation on the natural frequencies and load-frequency curves, a cantilever anti-symmetric angle-ply  $[\theta / -\theta]$  composite beam with  $L/h = 10$  is considered. The lowest three natural frequencies with and without the effect of axial force are given in Table 6. The corresponding mode shapes with fiber angles  $\theta = 30^\circ$  and  $60^\circ$  under a compressive axial force ( $P = 0.5P_{cr}$ ) are illustrated in Figs. 1 and 2. The mode shapes for other cases of axial force ( $P = 0$  and  $P = -0.5P_{cr}$ ) are similar to the corresponding ones for the case of axial force ( $P = 0.5P_{cr}$ ) and are not plotted, although there is a little difference between them. The change in the flexural natural frequencies due to axial force is significant for all fiber angles. It is noticed that these natural frequencies diminish as the axial force changes from tension ( $P = -0.5P_{cr}$ ) to compression ( $P = 0.5P_{cr}$ ). It reveals that the tension force has a stiffening effect while the compressive force has a softening effect on these natural frequencies. However, the third natural frequencies of fiber angles  $\theta = 60^\circ, 75^\circ$  and  $90^\circ$ , which correspond to the axial mode (Fig. 2c), are unaltered, as expected. The lowest three load-frequency curves with fiber angles  $\theta = 30^\circ$  and  $60^\circ$  are plotted in Figs. 3 and 4. The uncoupled solution, which neglects the coupling effects coming from the material anisotropy, are also given. Due to the small coupling effects (Figs. 1 and 2), the results by uncoupled and coupled solution are identical. Characteristic of load-frequency curves is that the value of the axial force for which the natural frequency vanishes constitutes the buckling load. Thus, for  $\theta = 60^\circ$ , the first flexural buckling occurs at  $P = 0.254$ . As a result, the lowest branch vanishes when  $P$  is slightly over this value. As the axial force increases, the second, third branch will also disappear when  $P$  is slightly over 2.195 and 5.568, respectively. It should be noted that for the third branch, two curves ( $P_{z_3} - \omega_{x_1}$ ) and ( $P_{z_3} - \omega_{z_3}$ ) intersect at  $P = 0.152$ , thus, after this value, the first axial mode becomes the third flexural one. A comprehensive three dimensional interaction diagram of the natural frequencies, axial compressive

force and fiber angle is plotted in Fig. 5. Three groups of curves are observed. The smallest group is for the first flexural mode and the larger ones are for the second and third flexural mode, respectively.

The next example is the same as before except that in this case, an unsymmetric  $[0^\circ/\theta]$  lay-up is considered. Major effects of the axial force on the natural frequencies are again seen in Table 7. Three dimensional interaction diagram between axial-flexural buckling and natural frequency with respect to the fiber angle change is shown in Fig. 6. Similar phenomena as the previous example can be observed except that in this case all three groups of curves are axial-flexural coupled mode. The lowest three load-frequency curves with fiber angles  $\theta = 45^\circ$  and  $75^\circ$  are displayed in Figs. 7 and 8. Due to strong coupling effects, the results by uncoupled and coupled solution show discrepancy. It can be explained partly by the normal mode shapes corresponding to the first three natural frequencies with fiber angle  $\theta = 75^\circ$  for the case of an axial compressive force ( $P = 0.5P_{cr}$ ) in Fig. 9. Relative measures of axial and flexural displacements show that all three modes are triply coupled vibration (axial, bending and shear components). That is, the uncoupled solution is no longer valid for unsymmetrically laminated beams, and triply axial-flexural coupled should be considered.

Finally, the effects of modulus ratio ( $E_1/E_2$ ) on the first load-frequency curve of a simply-supported composite beam with  $L/h = 10$  are investigated. A symmetric and an anti-symmetric cross-ply lay-ups are considered. It is observed from Fig. 10 that the fundamental natural frequencies and critical buckling loads as well as load-frequency curves increase with increasing orthotropy ( $E_1/E_2$ ) for two lay-ups considered.

## 8. Conclusions

A theoretical model is presented to study the axial-flexural coupled vibration of rectangular composite beams with arbitrary lay-ups under a constant axial force. This model is capable of predicting accurately the natural frequencies, critical buckling loads and load-frequency curves as well as corresponding mode shapes for various configurations. It accounts for the parabolical variation of shear strains through the depth of the beam, and satisfies the zero traction boundary conditions on the top and bottom surfaces of the beam without using shear correction factor. To formulate the problem, a one-dimensional displacement-based finite element method is employed. All of the possible vibration mode shapes including the axial and flexural mode as well as triply axial-flexural coupled mode are included in the analysis. The present model is found to be appropriate and efficient in analyzing free vibration problem of rectangular composite beams under a constant axial force.

## 9. References

### References

- [1] W. P. Howson, F. W. Williams, Natural frequencies of frames with axially loaded Timoshenko members, *Journal of Sound and Vibration* 26 (4) (1973) 503 – 515.
- [2] F. Y. Cheng, W. H. Tseng, Dynamic matrix of Timoshenko beam columns, *Journal of the Structural Division* 99 (3) (1973) 527–549.
- [3] K. Soldatos, I. Elishakoff, A transverse shear and normal deformable orthotropic beam theory, *Journal of Sound and Vibration* 155 (3) (1992) 528 – 533.
- [4] K. Chandrashekhara, K. Bangera, Free vibration of composite beams using a refined shear flexible beam element, *Computers and Structures* 43 (4) (1992) 719 – 727.
- [5] G. Shi, K. Y. Lam, Finite element vibration analysis of composite beams based on higher-order beam theory, *Journal of Sound and Vibration* 219 (4) (1999) 707 – 721.
- [6] S. R. Marur, T. Kant, Free vibration analysis of fiber reinforced composite beams using higher order theories and finite element modelling, *Journal of Sound and Vibration* 194 (3) (1996) 337 – 351.
- [7] S. R. Marur, T. Kant, On the angle ply higher order beam vibrations, *Computational Mechanics* 40 (2007) 25–33.
- [8] M. V. V. S. Murthy, D. R. Mahapatra, K. Badarinarayana, S. Gopalakrishnan, A refined higher order finite element for asymmetric composite beams, *Composite Structures* 67 (1) (2005) 27 – 35.
- [9] P. Subramanian, Dynamic analysis of laminated composite beams using higher order theories and finite elements, *Composite Structures* 73 (3) (2006) 342 – 353.
- [10] P. Vidal, O. Polit, A family of sinus finite elements for the analysis of rectangular laminated beams, *Composite Structures* 84 (1) (2008) 56 – 72.
- [11] L. Jun, L. Xiaobin, H. Hongxing, Free vibration analysis of third-order shear deformable composite beams using dynamic stiffness method, *Archive of Applied Mechanics* 79 (2009) 1083–1098.
- [12] E. Carrera, M. Petrolo, P. Nali, Unified formulation applied to free vibrations finite element analysis of beams with arbitrary section, *Shock and Vibration* 18 (3) (2011) 485–502.

- [13] L. Jun, H. Hongxing, Free vibration analyses of axially loaded laminated composite beams based on higher-order shear deformation theory, *Meccanica* 46 (2011) 1299–1317.
- [14] A. A. Khdeir, J. N. Reddy, Free vibration of cross-ply laminated beams with arbitrary boundary conditions, *International Journal of Engineering Science* 32 (12) (1994) 1971–1980.
- [15] A. A. Khdeir, J. N. Reddy, Buckling of cross-ply laminated beams with arbitrary boundary conditions, *Composite Structures* 37 (1) (1997) 1 – 3.
- [16] S. J. Song, A. M. Waas, Effects of shear deformation on buckling and free vibration of laminated composite beams, *Composite Structures* 37 (1) (1997) 33 – 43.
- [17] H. Matsunaga, Vibration and buckling of multilayered composite beams according to higher order deformation theories, *Journal of Sound and Vibration* 246 (1) (2001) 47 – 62.
- [18] M. Aydogdu, Vibration analysis of cross-ply laminated beams with general boundary conditions by Ritz method, *International Journal of Mechanical Sciences* 47 (11) (2005) 1740 – 1755.
- [19] M. Aydogdu, Buckling analysis of cross-ply laminated beams with general boundary conditions by Ritz method, *Composites Science and Technology* 66 (10) (2006) 1248 – 1255.
- [20] W. Zhen, C. Wanji, An assessment of several displacement-based theories for the vibration and stability analysis of laminated composite and sandwich beams, *Composite Structures* 84 (4) (2008) 337 – 349.
- [21] M. Karama, B. A. Harb, S. Mistou, S. Caperaa, Bending, buckling and free vibration of laminated composite with a transverse shear stress continuity model, *Composites Part B: Engineering* 29 (3) (1998) 223 – 234.
- [22] T. P. Vo, H.-T. Thai, Static behaviour of composite beams using various refined shear deformation theories, *Composite Structures* (2012) In Press.
- [23] R. M. Jones, *Mechanics of Composite Materials*, Taylor & Francis, 1999.

Figure 1: Vibration mode shapes of a cantilever anti-symmetric angle-ply composite beam with the fiber angle  $30^\circ$  under a axial compressive force ( $P = 0.5P_{cr}$ ).

Figure 2: Vibration mode shapes of a cantilever anti-symmetric angle-ply composite beam with the fiber angle  $60^\circ$  under a axial compressive force ( $P = 0.5P_{cr}$ ).

Figure 3: Effect of axial force on the first three natural frequencies with the fiber angle  $30^\circ$  of a cantilever anti-symmetric angle-ply composite beam.

Figure 4: Effect of axial force on the first three natural frequencies with the fiber angle  $60^\circ$  of a cantilever anti-symmetric angle-ply composite beam.

Figure 5: Three dimensional interaction diagram between the axial compressive force and the first three natural frequencies of a cantilever anti-symmetric angle-ply composite beam with respect to the fiber angle change.

Figure 6: Three dimensional interaction diagram between the axial compressive force and the first three natural frequencies of a cantilever unsymmetric composite beam with respect to the fiber angle change.

Figure 7: Effect of axial force on the first three natural frequencies with the fiber angle  $45^\circ$  of a cantilever unsymmetric composite beam.

Figure 8: Effect of axial force on the first three natural frequencies with the fiber angle  $75^\circ$  of a cantilever unsymmetric composite beam.

Figure 9: Vibration mode shapes of a cantilever unsymmetric composite beam with the fiber angle  $75^\circ$  under a axial compressive force ( $P = 0.5P_{cr}$ ).

Figure 10: Variation of the first load-frequency curves with respect to modulus ratio change of a simply-supported symmetric and anti-symmetric cross-ply composite beam.

1  
2  
3  
4  
5  
6  
7  
8  
9  
10  
11  
12  
13  
14  
15  
16  
17  
18  
19  
20  
21  
22  
23  
24  
25  
26  
27  
28  
29  
30  
31  
32  
33  
34  
35  
36  
37  
38  
39  
40  
41  
42  
43  
44  
45  
46  
47  
48  
49  
50  
51  
52  
53  
54  
55  
56  
57  
58  
59  
60  
61  
62  
63  
64  
65

Table 1: Effect of axial force on the first four natural frequencies of a simply-supported beam with a symmetric cross-ply  $[90^\circ/0^\circ/0^\circ/90^\circ]$  lay-up.

Table 2: Comparison of the first four non-dimensional natural frequencies of symmetric cross-ply composite beams with various boundary conditions.

Table 3: Comparison of the first four non-dimensional natural frequencies of simply-supported anti-symmetric cross-ply composite beams.

Table 4: Comparison of the non-dimensional fundamental natural frequencies of symmetric and anti-symmetric cross-ply composite beams with various boundary conditions.

Table 5: Comparison of the non-dimensional critical buckling loads of symmetric and anti-symmetric cross-ply composite beams with various boundary conditions.

Table 6: Effect of axial force on the first three non-dimensional natural frequencies of a cantilever anti-symmetric angle-ply  $[\theta/-\theta]$  composite beam with respect to the fiber angle change.

Table 7: Effect of axial force on the first three non-dimensional natural frequencies of an unsymmetric  $[0^\circ/\theta]$  cantilever composite beam with respect to the fiber angle change.

## CAPTIONS OF TABLES

Table 1: Effect of axial force on the first four natural frequencies of a simply-supported beam with a symmetric cross-ply  $[90^0 / 0^0 / 0^0 / 90^0]$  lay-up.

Table 2: Comparison of the first four non-dimensional natural frequencies of symmetric cross-ply composite beams with various boundary conditions.

Table 3: Comparison of the first four non-dimensional natural frequencies of simply-supported anti-symmetric cross-ply composite beams.

Table 4: Comparison of the non-dimensional fundamental natural frequencies of symmetric and anti-symmetric cross-ply composite beams with various boundary conditions.

Table 5: Comparison of the non-dimensional critical buckling loads of symmetric and anti-symmetric cross-ply composite beams with various boundary conditions.

Table 6: Effect of axial force on the first three non-dimensional natural frequencies of a cantilever anti-symmetric angle-ply  $[\theta / -\theta]$  composite beam with respect to the fiber angle change.

Table 7: Effect of axial force on the first three non-dimensional natural frequencies of an unsymmetric  $[0 / \theta]$  cantilever composite beam with respect to the fiber angle change.



Table 1: Effect of axial force on the first four natural frequencies of a simply-supported beam with a symmetric cross-ply  $[90^0 / 0^0 / 0^0 / 90^0]$  lay-up.

Mode	$P = 10^9 \text{ N}$			$P = 0$			$P = -10^9 \text{ N}$	
	(compression)			(no axial force)			(tension)	
	ABAQUS [21]	Ref. [21]	Present	ABAQUS [21]	Ref. [21]	Ref. [10]	Present	Present
1	78.60	77.00	75.63	82.90	83.70	82.78	82.42	88.69
2	195.05	184.44	183.95	200.60	195.80	195.83	195.20	205.83
3	317.09	297.76	300.54	324.30	313.40	311.73	315.88	330.50
4	441.11	422.44	431.19	450.1	441.80	428.96	449.83	467.72

Table 2: Comparison of the first four non-dimensional natural frequencies of symmetric cross-ply composite beams with various boundary conditions.

Mode	Simply-supported		Cantilever- Free		Clamped-Clamped	
	Marur and Kant [7]	Present	Marur and Kant [7]	Present	Marur and Kant [7]	Present
1	2.3094	2.3138	0.8846	0.8866	3.7090	3.7715
2	6.9808	7.0091	4.1214	4.1716	7.8271	8.3662
3	12.0500	12.1250	9.0231	9.1787	12.5878	12.9934
4	17.1358	17.2949	<b>11.4422*</b>	<b>11.4721*</b>	17.5105	18.2571

\*: Axial natural frequencies; rest ones are flexural natural frequencies

Table 3: Comparison of the first four non-dimensional natural frequencies of simply-supported anti-symmetric cross-ply composite beams.

Mode	Reference	L/h		
		5	10	20
1	Vidal and Polit [10]	4.78	5.29	5.45
	ANSYS [10]	4.77	5.29	5.45
	Present	4.76	5.28	5.45
2	Vidal and Polit [10]	14.71	19.14	21.20
	ANSYS [10]	14.61	19.12	21.18
	Present	14.56	19.03	21.14
3	Vidal and Polit [10]	25.87	37.87	45.62
	ANSYS [10]	25.40	37.77	45.55
	Present	27.21	36.44	45.32
4	Vidal and Polit [10]	35.56	58.97	76.81
	ANSYS [10]	35.42	58.60	76.59
	Present	39.60	61.08	74.65

Table 4: Comparison of the non-dimensional fundamental natural frequencies of symmetric and anti-symmetric cross-ply composite beams with various boundary conditions.

Lay-ups	Reference	L/h		
		5	10	20
<i>Simply-supported beam</i>				
[0 <sup>0</sup> /90 <sup>0</sup> /0 <sup>0</sup> ]	Murthy et al. [8]	9.207	13.614	-
	Khdeir and Reddy [14]	9.208	13.614	-
	Aydogdu [18]	9.207	-	16.337
	Present	9.206	13.607	16.327
[0 <sup>0</sup> /90 <sup>0</sup> ]	Khdeir and Reddy [14]	6.128	6.945	-
	Aydogdu [18]	6.144	-	7.218
	Present	6.058	6.909	7.204
<i>Cantilever- Free beam</i>				
[0 <sup>0</sup> /90 <sup>0</sup> /0 <sup>0</sup> ]	Murthy et al.[8]	4.230	5.491	-
	Khdeir and Reddy[14]	4.234	5.495	-
	Aydogdu[18]	4.233	-	6.070
	Present	4.230	5.490	6.062
[0 <sup>0</sup> /90 <sup>0</sup> ]	Murthy et al.[8]	2.378	2.541	-
	Khdeir and Reddy [14]	2.386	2.544	-
	Aydogdu [18]	2.384	-	2.590
	Present	2.381	2.541	2.589
<i>Clamped-Clamped beam</i>				
[0 <sup>0</sup> /90 <sup>0</sup> /0 <sup>0</sup> ]	Murthy et al. [8]	11.602	19.719	
	Khdeir and Reddy [14]	11.603	19.712	-
	Aydogdu [18]	11.637	-	29.926
	Present	11.601	19.708	29.643
[0 <sup>0</sup> /90 <sup>0</sup> ]	Murthy et al. [8]	10.011	13.657	-
	Khdeir and Reddy [14]	10.026	13.660	-
	Aydogdu [18]	10.103	-	15.688
	Present	10.022	13.659	15.650

Table 5: Comparison of the non-dimensional critical buckling loads of symmetric and anti-symmetric cross-ply composite beams with various boundary conditions.

Lay-ups	Reference	L/h		
		5	10	20
<i>Simply-supported beam</i>				
[0 <sup>0</sup> /90 <sup>0</sup> /0 <sup>0</sup> ]	Khdeir and Reddy [15]	8.613	18.832	-
	Aydogdu [19]	8.613	-	27.084
	Present	8.609	18.814	27.050
[0 <sup>0</sup> /90 <sup>0</sup> ]	Aydogdu [19]	3.906	-	5.296
	Present	3.903	4.936	5.290
<i>Cantilever- Free beam</i>				
[0 <sup>0</sup> /90 <sup>0</sup> /0 <sup>0</sup> ]	Khdeir and Reddy [15]	4.708	6.772	-
	Aydogdu [19]	4.708	-	7.611
	Present	4.704	6.762	7.600
[0 <sup>0</sup> /90 <sup>0</sup> ]	Aydogdu [19]	1.236	-	1.349
	Present	1.234	1.322	1.347
<i>Clamped-Clamped beam</i>				
[0 <sup>0</sup> /90 <sup>0</sup> /0 <sup>0</sup> ]	Khdeir and Reddy [15]	11.652	34.453	-
	Present	11.648	34.437	75.257
[0 <sup>0</sup> /90 <sup>0</sup> ]	Present	8.670	15.619	19.757

Table 6: Effect of axial force on the first three non-dimensional natural frequencies of a cantilever anti-symmetric angle-ply  $[\theta / -\theta]$  composite beam with respect to the fiber angle change.

Fiber angle	Buckling loads	P=-0.5P <sub>cr</sub> (tension)			P=0 (no axial force)			P=0.5P <sub>cr</sub> (compression)		
		$\omega_1$	$\omega_2$	$\omega_3$	$\omega_1$	$\omega_2$	$\omega_3$	$\omega_1$	$\omega_2$	$\omega_3$
0	7.065	6.674	25.357	51.890	5.625	23.553	49.648	4.144	21.575	47.293
15	6.525	6.082	23.747	49.286	4.971	21.938	47.108	3.270	19.938	44.818
30	1.581	3.322	15.589	35.930	2.771	14.864	35.201	2.009	14.095	34.457
45	0.462	1.818	9.288	23.308	1.512	8.907	22.965	1.092	8.506	22.617
60	0.254	1.350	7.033	17.500*	1.122	6.751	17.500*	0.810	6.455	17.500*
75	0.212	1.234	6.450	15.980*	1.026	6.193	15.980*	0.740	5.923	15.980*
90	0.205	1.213	6.345	15.709*	1.008	6.092	15.709*	0.728	5.826	15.709*

\*: Axial natural frequencies; rest ones are flexural natural frequencies.

Table 7: Effect of axial force on the first three non-dimensional natural frequencies of an unsymmetric  $[0/\theta]$  cantilever composite beam with respect to the fiber angle change.

Fiber angle	Buckling loads	P = -0.5P <sub>cr</sub> (tension)			P = 0 (no axial force)			P = 0.5P <sub>cr</sub> (compression)		
		$\omega_1$	$\omega_2$	$\omega_3$	$\omega_1$	$\omega_2$	$\omega_3$	$\omega_1$	$\omega_2$	$\omega_3$
0	7.065	6.674	25.357	51.890	5.625	23.553	49.648	4.144	21.575	47.293
15	6.149	6.274	24.376	50.393	5.281	22.734	48.389	3.882	20.941	46.293
30	3.081	4.572	19.911	43.687	3.826	18.856	42.533	2.786	17.726	41.345
45	1.694	3.440	16.224	37.675	2.869	15.477	36.934	2.079	14.685	36.177
60	1.395	3.131	15.059	35.574	2.609	14.387	34.925	1.889	13.677	34.264
75	1.333	3.062	14.776	35.015	2.551	14.120	34.385	1.847	13.427	33.742
90	1.322	3.050	14.722	34.899	2.541	14.069	34.271	1.839	13.379	33.632

## CAPTIONS OF FIGURES

Figure 1: Vibration mode shapes with the axial and flexural components of a cantilever anti-symmetric angle-ply composite beam with the fiber angle  $30^0$

Figure 2: Vibration mode shapes with the axial and flexural components of a cantilever anti-symmetric angle-ply composite beam with the fiber angle  $60^0$

Figure 3: Effect of axial force on the first three natural frequencies with the fiber angle  $30^0$  of a cantilever anti-symmetric angle-ply composite beam.

Figure 4: Effect of axial force on the first three natural frequencies with the fiber angle  $60^0$  of a cantilever anti-symmetric angle-ply composite beam.

Figure 5: Three dimensional interaction diagram between the axial compressive force and the first three natural frequencies of a cantilever anti-symmetric angle-ply composite beam with respect to the fiber angle change.

Figure 6: Three dimensional interaction diagram between the axial compressive force and the first three natural frequencies of a cantilever unsymmetric composite beam with respect to the fiber angle change.

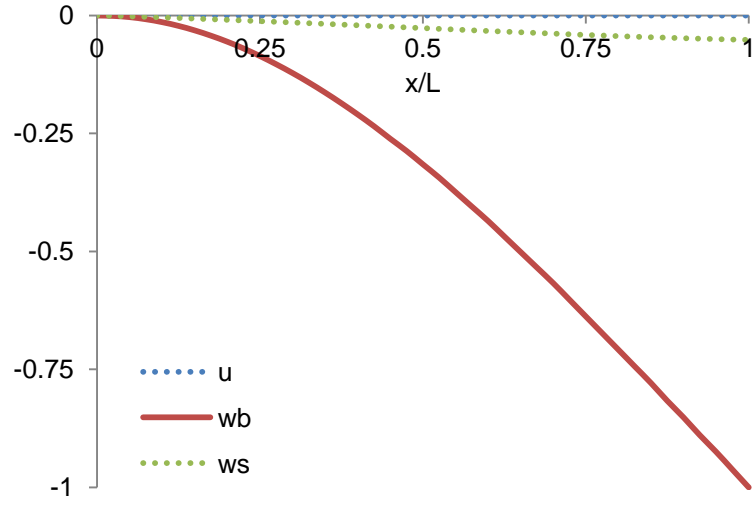
Figure 7: Effect of axial force on the first three natural frequencies with the fiber angle  $45^0$  of a cantilever un-symmetric composite beam.

Figure 8: Effect of axial force on the first three natural frequencies with the fiber angle  $75^0$  of a cantilever unsymmetric composite beam.

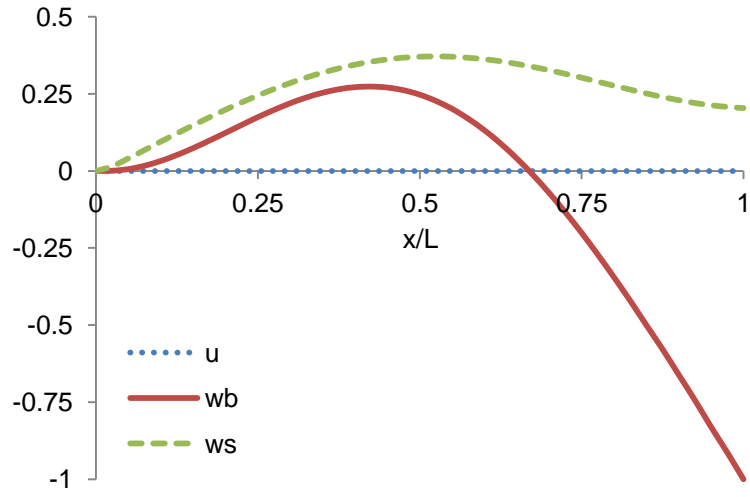
Figure 9: Vibration mode shapes with the axial and flexural components of a cantilever un-symmetric composite beam with the fiber angle  $75^0$ .

Figure 10: Variation of the first load-frequency curves with respect to modulus ratio change of a simply-supported symmetric and anti-symmetric cross-ply composite beam.

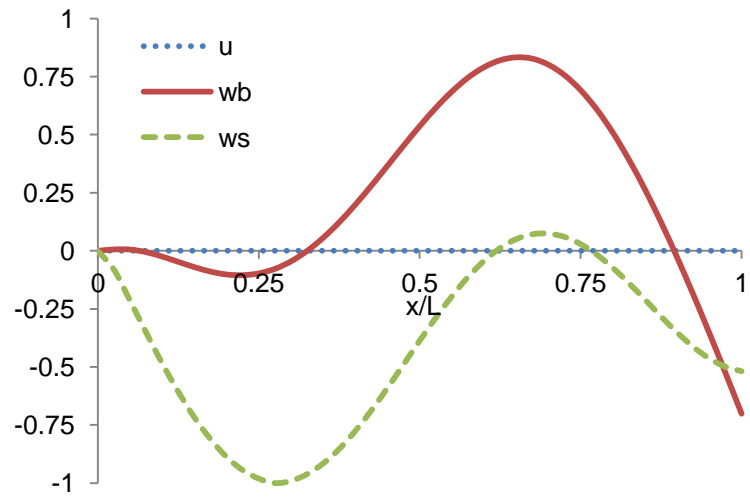




a. Fundamental mode shape  $\omega_1 = 2.009$

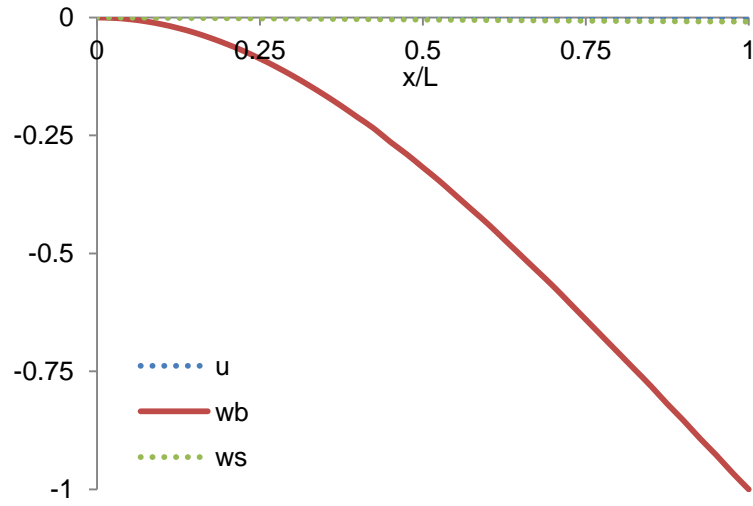


b. Second mode shape  $\omega_2 = 14.095$

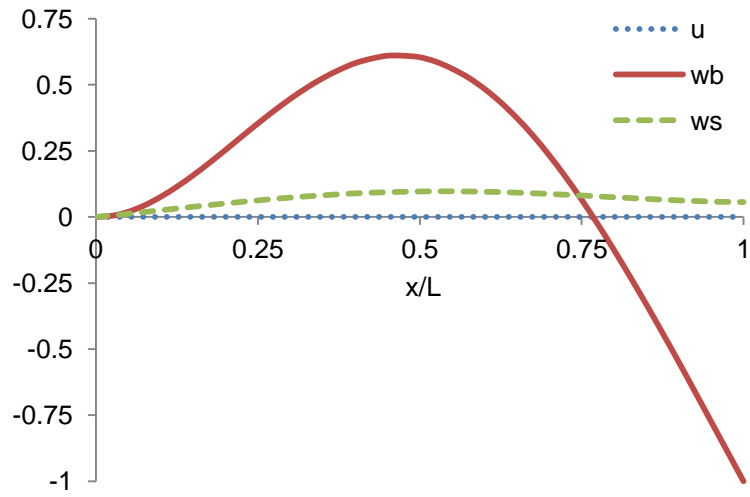


c. Third mode shape  $\omega_3 = 34.457$

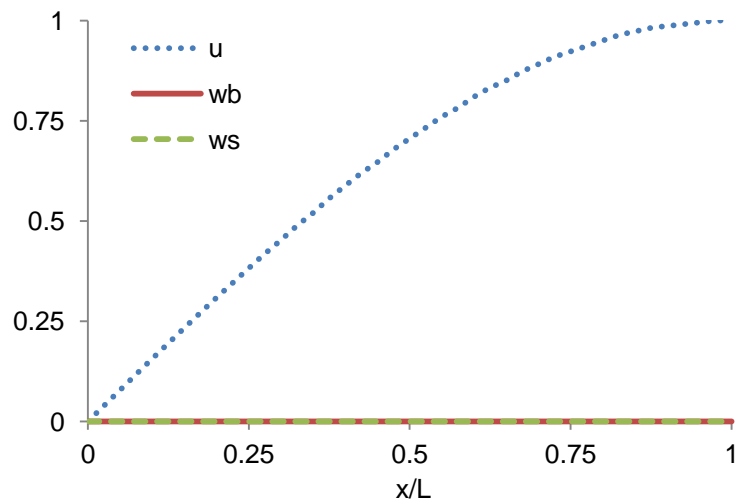
Figure 1: Vibration mode shapes with the axial and flexural components of a cantilever anti-symmetric angle-ply composite beam with the fiber angle  $30^\circ$



a. Fundamental mode shape  $\omega_1 = 0.810$



b. Second mode shape  $\omega_2 = 6.455$



c. Third mode shape  $\omega_3 = 17.500$

Figure 2: Vibration mode shapes with the axial and flexural components of a cantilever anti-symmetric angle-ply composite beam with the fiber angle  $60^\circ$

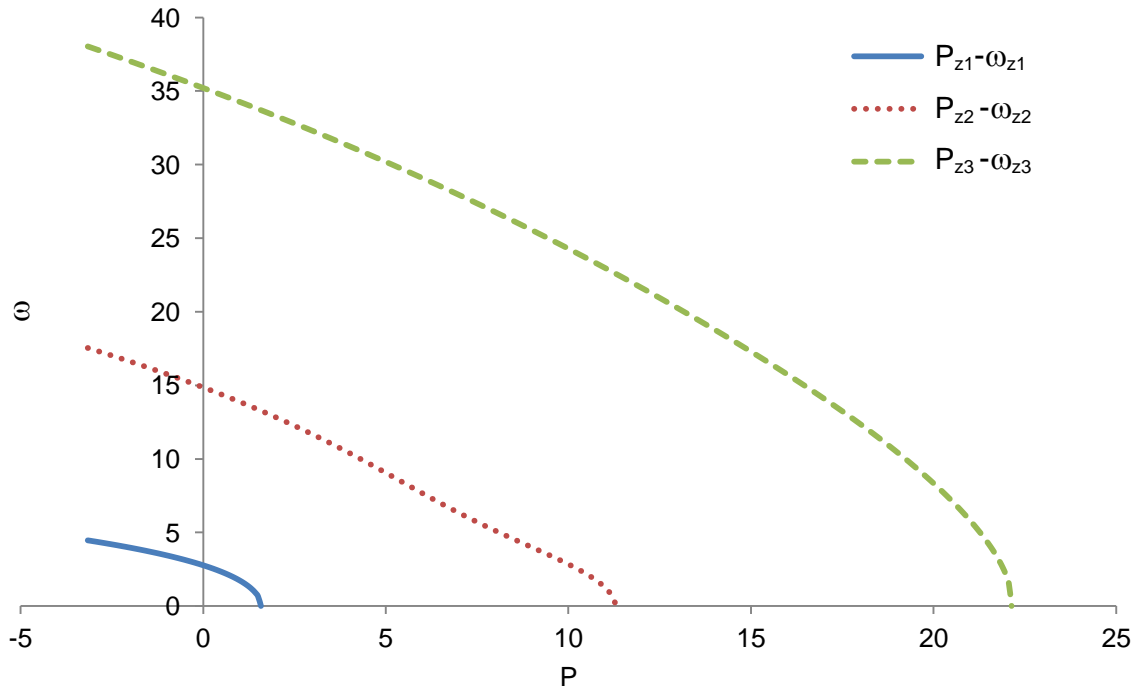


Figure 3: Effect of axial force on the first three natural frequencies with the fiber angle  $30^\circ$  of a cantilever anti-symmetric angle-ply composite beam.

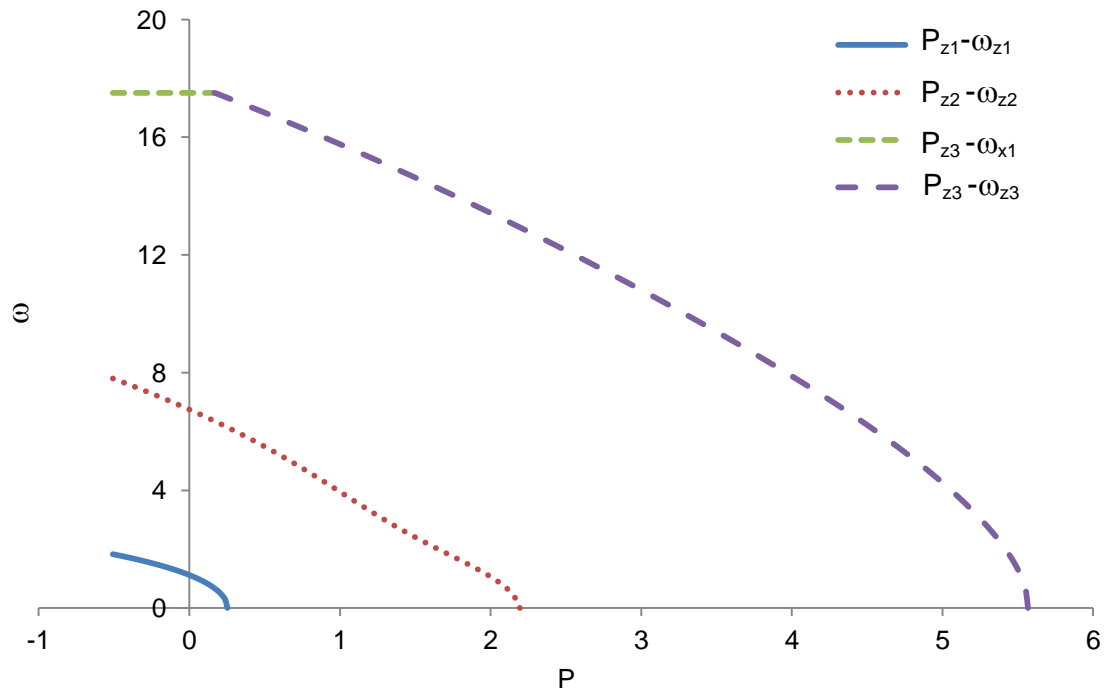


Figure 4: Effect of axial force on the first three natural frequencies with the fiber angle  $60^\circ$  of a cantilever anti-symmetric angle-ply composite beam.

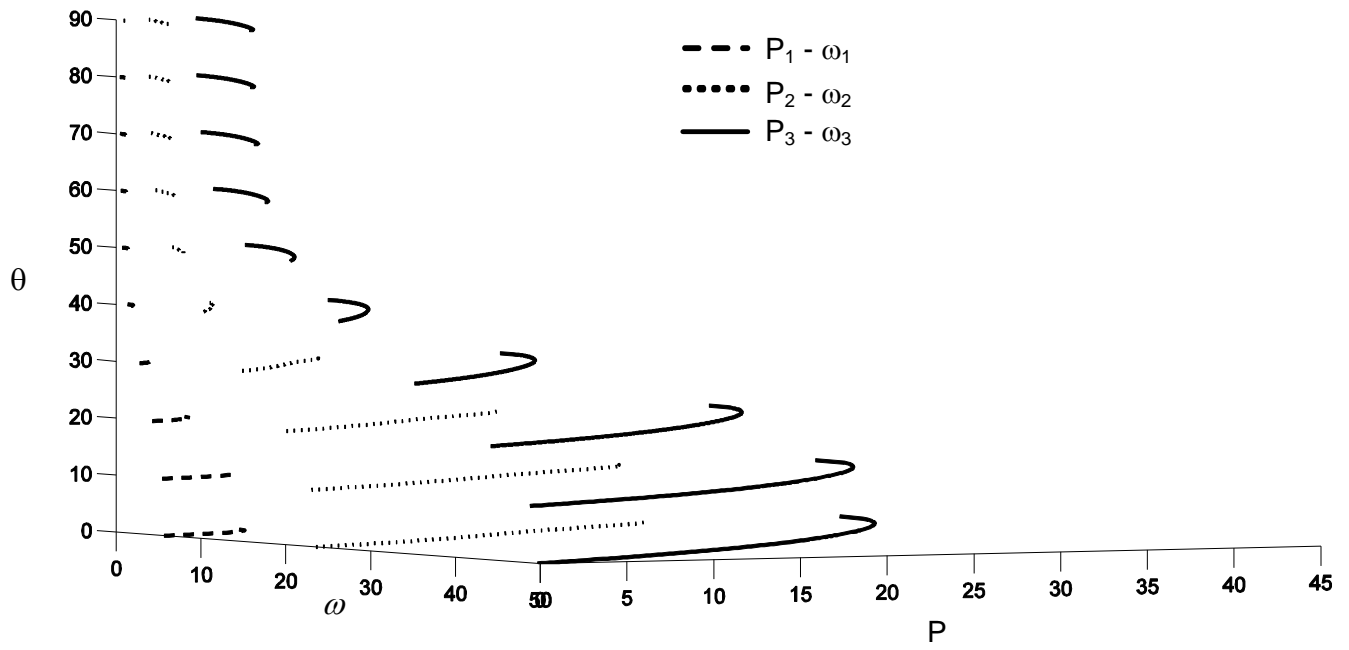


Figure 5: Three dimensional interaction diagram between the axial compressive force and the first three natural frequencies of a cantilever anti-symmetric angle-ply composite beam with respect to the fiber angle change.

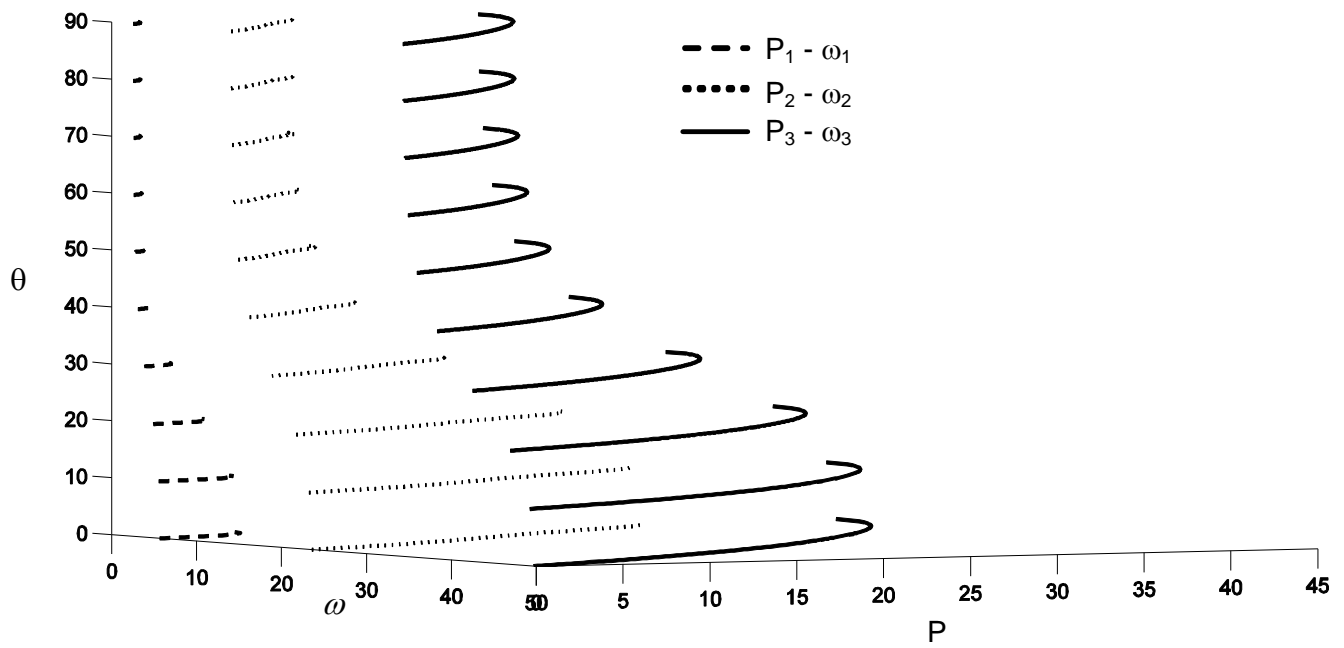


Figure 6: Three dimensional interaction diagram between the axial compressive force and the first three natural frequencies of a cantilever unsymmetric composite beam with respect to the fiber angle change.

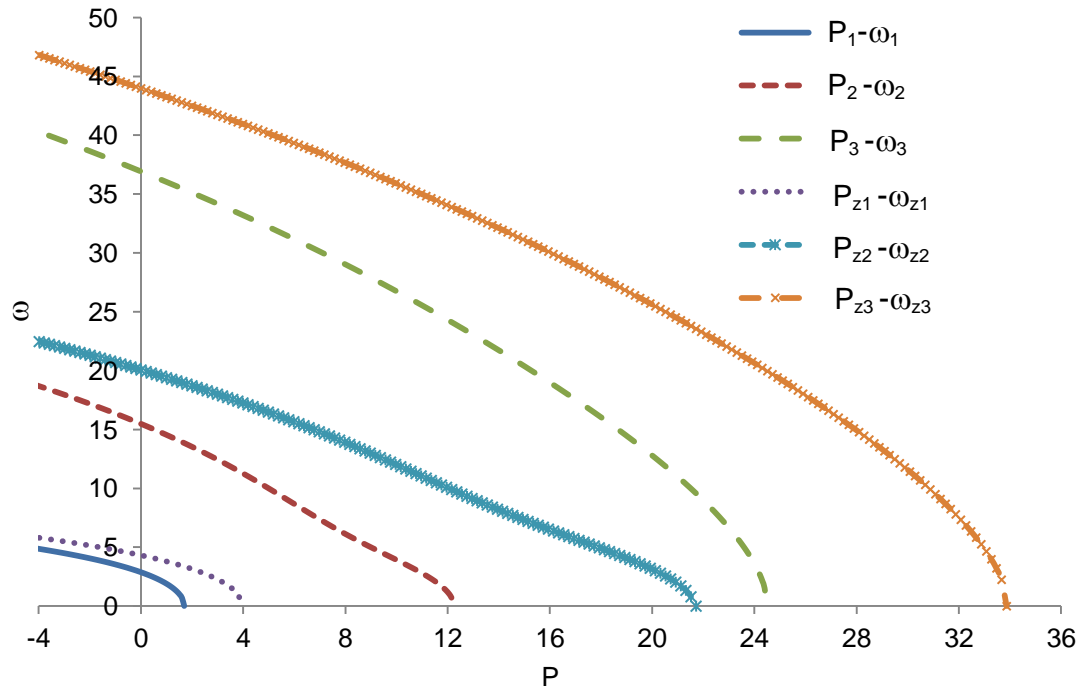


Figure 7: Effect of axial force on the first three natural frequencies with the fiber angle  $45^\circ$  of a cantilever un-symmetric composite beam.

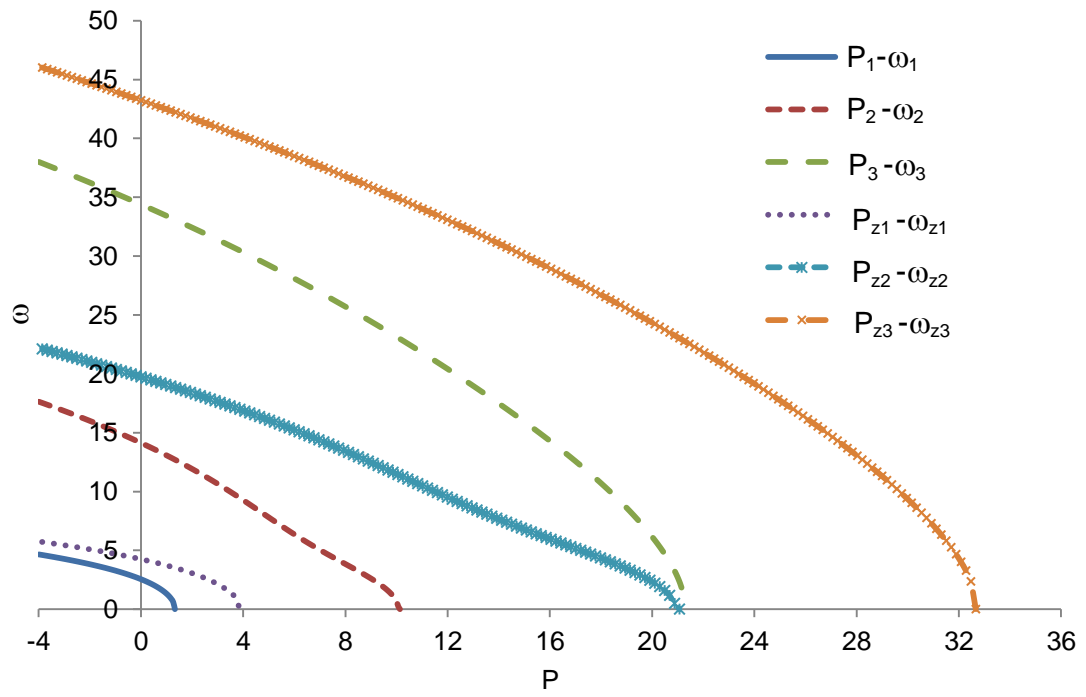
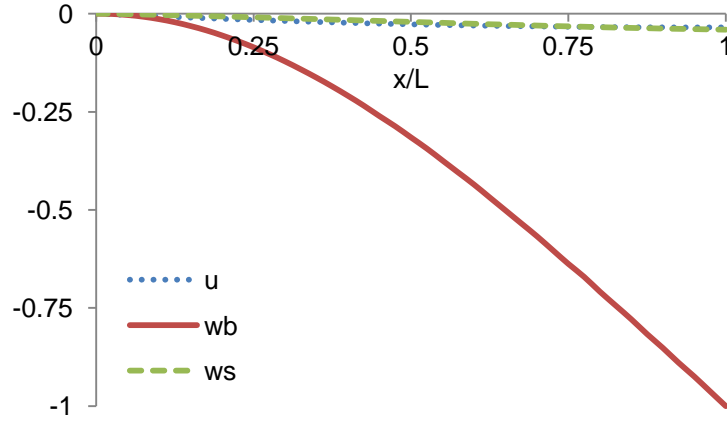
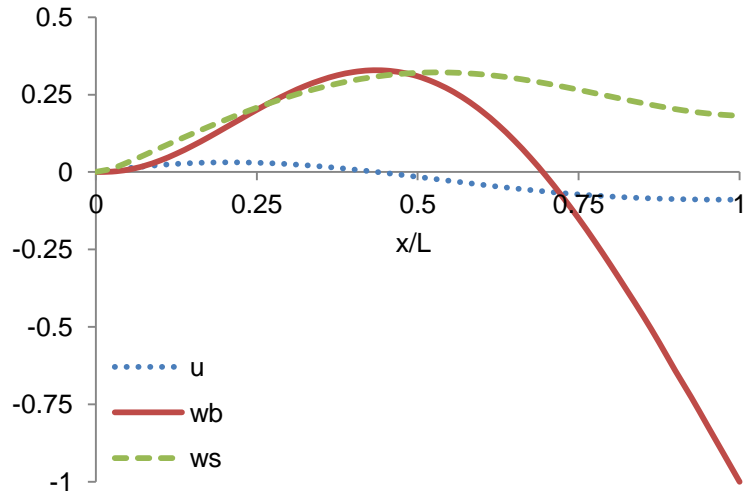


Figure 8: Effect of axial force on the first three natural frequencies with the fiber angle  $75^\circ$  of a cantilever unsymmetric composite beam.

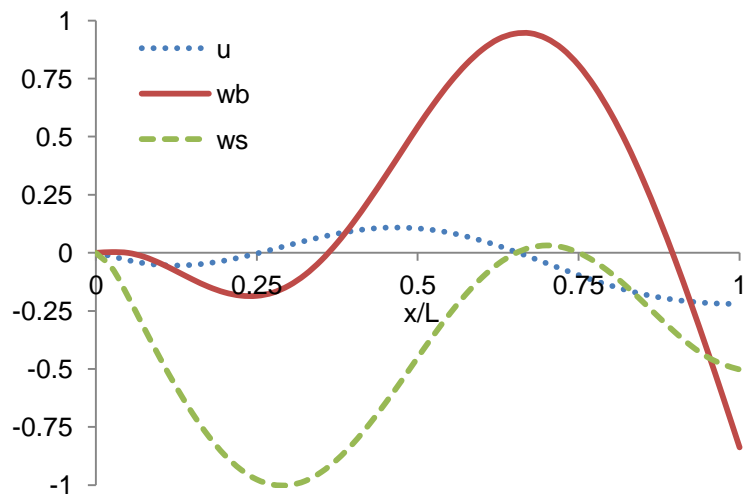




a. Fundamental mode shape  $\omega_1 = 1.847$ .



b. Second mode shape  $\omega_2 = 13.427$ .



c. Third mode shape  $\omega_3 = 33.742$ .

Figure 9: Vibration mode shapes with the axial and flexural components of a cantilever unsymmetric composite beam with the fiber angle  $75^\circ$ .

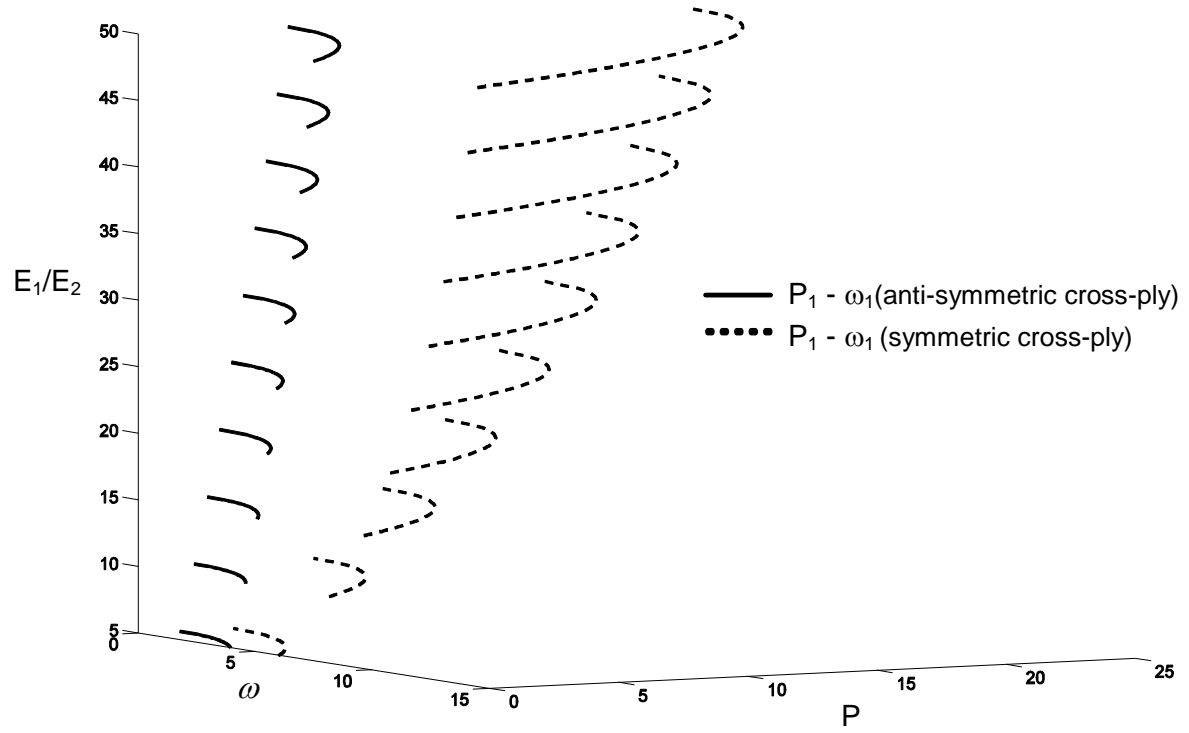


Figure 10: Variation of the first load-frequency curves with respect to modulus ratio change of a simply-supported symmetric and anti-symmetric cross-ply composite beam.